Comparing the Conformational Behavior of a Series of Diastereomeric Cyclic Urea HIV-1 Inhibitors Using the Low Mode:Monte Carlo Conformational Search Method

Carol A. Parish,* Matthew Yarger, Kent Sinclair, Myrianne Dure, and Alla Goldberg

Department of Chemistry, Hobart and William Smith Colleges, Geneva, New York 14456

Received April 13, 2004

The conformational flexibility of a series of diastereomeric cyclic urea HIV-1 protease inhibitors has been examined using the Low Mode:Monte Carlo conformational search method. Force fields were validated by a comparison of the energetic ordering of the minimum energy structures on the AMBER*/GBSA(water), OPLSAA/GBSA(water) and HF/6-311G**/SCRF(water) surfaces. The energetic ordering of the minima on the OPLSAA /GBSA(water) surface was in better agreement with the quantum calculations than the ordering on the AMBER*/GBSA(water) surface. An ensemble of low energy structures was generated using OPLSAA/GBSA(water) and used to compare the molecular shape and flexibility of each diastereomer to the experimentally determined binding affinities and crystal structures of closely related systems. The results indicate that diastereomeric solution-phase energetic stability, conformational rigidity and ability to adopt a chair conformation correlate strongly with experimental binding affinities. Rigid body docking suggests that all of the diastereomers adopt solution-phase conformations suitable for alignment with the HIV-1 protease; however, these results indicate that the binding affinities are dependent upon subtle differences in the P1/P1′ and P2/P2′ substituent orientations.

Introduction

The human immunodeficiency virus (HIV) encodes an aspartyl protease enzyme that cleaves viral polyprotein precursors, allowing the maturation of the HIV virus that causes the autoimmune deficiency disease (AIDS). The development of inhibitors of the HIV-1 protease has been the subject of intense effort and many excellent reviews are available.[1−15] A significant number of compounds, which are highly potent HIV-1 protease inhibitors, has been developed; however, the need to develop even better drug candidates is an ongoing effort due in part to the ability of the protease to mutate into drug-resistant forms.

Potent inhibitors interact with the HIV-1 protease through a series of electrostatic and steric interactions. One such interaction in many inhibitors is the formation of hydrogen bonds with the symmetrically equivalent pair of isoleucines (ILE 50 and 50′) near the flap region at the top of the active site by coordination through a crystallographically important water molecule.[1] However, a series of potent cyclic urea inhibitors were designed to displace the structural water and to provide a compact, rigid structure that maximizes tight binding interactions with the protease.[8,16−41] At least two systems, DMP323 and DMP450, were viable drug candidates only to be discontinued due to high blood level variability in humans (DMP323)[20] and disappointing antiviral potency in the presence of plasma proteins (DMP450).[32] In an effort to understand the role of stereochemistry on binding, Kaltenbach and co-workers synthesized nine stereoisomers of the cyclic urea shown in Figure 1 and reported the associated binding affinities of each synthetically accessible stereoisomer[25] (Table 1). While it appears that drugs based upon the cyclic urea template, such as DMP450, are no longer in active clinical development, the elegance of the molecular design and the availability of experimental binding affinities inspired us to use these systems to (1) ask fundamental questions about the relationship between

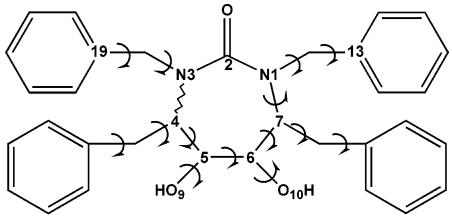

1

Figure 1. (4*,5*,6*,7*)-Hexahydro-5,6-dihydroxy-1,3,4,7-tetrakis(phenylmethyl)-2*H*-1,3-diazapin-2-one. Degrees of freedom varied during the conformational searches are shown with arrows and the wavy line indicates the bond used to open the ring for interconversion of ring conformations.

Table 1. Experimental Binding Affinities of the Cyclic Urea Diastereomers of **1**[25]

isomer configuration C4−C5−C6−C7	K_i (nM)
RSSR	3.6
SRRS	3810
RRRR	1350
SSSS	560
RSRR	6.4
SRRR	6700
RSRR	6.0
SRSS	1710
RSRS	250

* To whom correspondence should be addressed. E-mail: parish@hws.edu, Telephone: (315) 781-3607, Fax: (315) 781-3860.

10.1021/jm049716l CCC: $27.50
Published on Web 08/31/2004

molecular flexibility and function, (2) evaluate the predictability of the molecular mechanics treatment and (3) evaluate the ability of the Low Mode:Monte Carlo (LM:MC) conformational searching method to exhaustively sample the resulting 14-dimensional potential energy surface.

Biological, physical and chemical properties depend on the nature of the accessible conformations.[42] We were interested in comparing the conformational flexibility of these cyclic urea systems. The identification of all low energy, conformationally accessible states yields information about molecular flexibility and conformational behavior, two concepts that are important in understanding inhibitor binding. For the results of a conformational search to be representative of the actual behavior of a molecular system, three criteria must be satisfied.[43,44] First, the molecular potential energy surface (PES) upon which the search takes place must be well defined and include environmental effects such as solvent. Many conformational search techniques are performed on surfaces generated using molecular mechanics force fields. In these cases, it is necessary to evaluate the accuracy of the force field used to represent the molecular system under study. Second, conformational sampling methods must be highly efficient and able to locate all low energy structures on the PES in a reasonable amount of computing time. Conformational search results may not be representative of the molecular behavior and flexibility if the method is only able to sample part of the multidimensional potential energy surface. Third, reasonable convergence criteria should be used to determine if a search is exhaustive. Searches started from different points on the PES must identify the same set of low energy structures, and the results must be time invariant; i.e., searches must be run until no new structures are found.

A variety of efficient conformational searching methods are available using simulated annealing,[5−7] distance geometry,[45−49] Monte Carlo[50−55] and eigenvector following[56−58] algorithms. Comprehensive reviews of conformational searching algorithms have been published elsewhere.[42,59−61] This study employs the Low Mode[56,57] (LM) and Monte Carlo[52] (MC) conformational search methods as they are implemented in the MacroModel/Maestro molecular modeling software program.[62] This method has been shown to be highly efficient in sampling the potential energy surfaces of diverse molecules.[63] In the combination method, explicit MC torsional rotation is combined with LM movement along the minimum energy paths that connect low energy structures, dovetailing the local exploration strengths of LM with the random surface "hopping" capability of MC.

This study will compare the solution phase conformational behavior of the 10 possible stereoisomers of **1**, nine of which have been synthesized and exhibit very different experimental HIV protease binding affinities. The LM:MC conformational search technique will be used to sample exhaustively the potential energy surface. While a significant number of energetic[16,34,35,38,64−70] and QSAR[67,71−75] studies of various cyclic ureas have been reported, to our knowledge this is the first report to describe the ensembles of low energy structures for a diastereomeric cyclic urea series.

Methods

The conformational ensembles that are generated in this study were calculated using version V7.2 of the MacroModel[62] suite of software programs running on 800 MHz Athlon PCs under the RedHat LINUX 6.2 operating system. Quantum calculations were performed with Jaguar V4.0.[76]

Conformational Searches. The Low Mode (LM) search method[56,57] was used in a 1:1 combination[63] with the Monte Carlo (MC) search method[52] to explore the potential energy surfaces of the stereoisomers of **1**. Each MC conformational search step varied a random number of torsional degrees of freedom between a minimum of two and a maximum of fourteen, where fourteen is the total number of variable torsion angles as shown in Figure 1. LM frequencies corresponding to the 10 lowest eigenvectors were explored. The total traveling distance for each step was selected randomly between 3 and 6 Å. Interconversion of ring structures was enabled using the ring-opening method of Still.[77,78] The *wavy* bond in Figure 1 is used for opening the seven-membered ring in each diastereomer. Starting structure chirality was preserved throughout the conformational searching. Searches were run in multiple blocks of 5000 LM:MC steps until they had reached convergence. Convergence was judged by monitoring the (1) energy of the most stable structure, (2) number of times this structure was visited, and (3) number of unique conformations found within 25.0 kJ mol^{-1} of the lowest energy minimum. Unique conformations were determined by superimposition of all heavy (non-hydrogen) atoms as well as reflection and/or rotation of the atom-numbering scheme. Structures were considered to be duplicates and rejected if the maximum interatomic distance was 0.25 Å or less following optimal RMS superposition. Structures that were found in previous searches were used to seed subsequent searches. Searches utilized the usage-directed structure selection method[52] that identifies the least used structure from among all known conformations and then uses this structure as the starting point for each new search. This ensures that a variety of different starting structures from different regions of the potential energy surface are used to begin each search. During the conformational search all structures were subjected to 1500 steps of the Truncated Newton Conjugate Gradient (TNCG)[79] minimization method to within a derivative convergence criterion of 0.01 kJ $Å^{-1}$ mol^{-1}.

Clustering Ensembles. Ensembles generated for each of the 10 stereoisomers were grouped into geometrically similar families using the XCluster[80] program. XCluster calculates the pairwise distance between each structure, in either torsional or Cartesian space, and partitions the conformations into geometrically similar subsets in an agglomerative, hierarchical fashion. The process begins with every structure as the only member of its own cluster. Individual structures are then grouped into clusters using the shortest distance between points as the threshold distance. At each clustering level the next shortest distance is used to form new, agglomerative clusters, with later clusters formed from groupings of earlier clusters. This process continues until all structures are a member of the same final cluster. The goal is to find the clustering level at which the distance between members of clusters is much smaller than the distance between clusters, i.e., the minimum separation ratio. Separation ratios greater than 2 that occur at high clustering level indicate significant clustering.[80] For a given clustering level, the full distance matrix was used to visualize the clustering of molecular structures in each ensemble. The clustering mosaics were used to illustrate how the clusters agglomerated as the clustering proceeded from the first level to the N-1 level.

Results and Discussion

Four contiguous chiral centers give rise to 10 stereoisomers. Of these 10 stereoisomers there are four enantiomeric pairs, *RRRR*/*SSSS*, *RSSR*/*SRRS*, *RSSS*/*RRRS* and *RSRR*/*SSRS*, and six unique diastereomers in an achiral environment (*RRRR*, *RSSR*, *RSSS*, *RSRR*,

Table 2. LM:MC Conformational Search Results within a 25 kJ mol^{-1} Energetic Window of the Lowest Energy Structure for Unique Diastereomers of **1**

	R R R R	*R R R S*	*R R S R*	*R R S S*	*R S R R*	*R S R S*	*R R S R*	*R R S S*	*R S R R*	*R S R S*	*R S S R*	*R S S S*	*R R S R*	*R R S S*	*R S R R*	*R S R S*	*R S S R*	*R S S S*
number of steps	number of conformations found						number of lowest minimum visits						minimum energy (kJ mol^{-1})					
5000	19	42	17	80	28	8	67	28	46	97	27	518	54.6	72.5	46.0	66.4	61.8	24.9
5000	22	45	17	82	28	8	191	91	139	211	63	1033	54.6	72.5	46.0	66.4	61.8	24.9
5000	20	45	17	81	28	8	201	156	223	305	88	1552	54.6	72.5	46.0	66.4	61.8	24.9
5000	19	45	18	82	28	8	236	217	306	406	118	2101	54.6	72.5	46.0	66.4	61.8	24.9
5000	20	44	18	82	28	8	247	260	373	496	154	2648	54.6	72.5	46.0	66.4	61.8	24.9
5000	19	44	18	82	28	8	251	310	442	610	183	3151	54.6	72.5	46.0	66.4	61.8	24.9
5000	20	45	18	82	28	8	271	385	509	670	212	3666	54.6	72.5	46.0	66.4	61.8	24.9
5000	19	45	18	82	28	8	280	462	588	796	250	4202	54.6	72.5	46.0	66.4	61.8	24.9
5000	19	44	18	83	28	8	296	504	679	985	278	4679	54.6	72.5	46.0	66.4	61.8	24.9
5000	19	45	18	83	28	8	314	568	742	1085	299	5211	54.6	72.5	46.0	66.4	61.8	24.9
5000	19	45	18	82	28	8	319	647	815	1176	326	5704	54.6	72.5	46.0	66.4	61.8	24.9
Total: 55 000	19	45	18	82	28	8	319	647	815	1176	326	5704	54.6	72.5	46.0	66.4	61.8	24.0

RSRS and *RRSS*). In this study, we will investigate the conformational flexibility of these diastereomers.

Generating Potential Energy Surfaces. Seven different force fields are available in the MacroModel program. It is important to choose a force field that is well parametrized for the molecular system under study. Accurate torsional parameters are particularly important in flexible molecular systems since they control conformational interconversions. AMBER*[81] and OPLSAA,[82,83] as implemented in MacroModel V7.2, contained the fewest low quality torsion parameters for the cyclic urea stereoisomers, and these force fields were used without modification. Solvent effects were included using the Generalized Born/Surface Area (GBSA) continuum model[84−89] for water. GBSA has been shown to reproduce accurately the hydration free energies for various molecular systems.[86] Nonbonded interactions within 8 Å for van der Waals' and 20 Å for electrostatic interactions were included in all calculations employing the GBSA model.

Initially the AMBER* force field was utilized, along with the GBSA(water) model, because the AMBER* method is capable of performing united-atom calculations where hydrogens on carbon atoms are not explicitly considered but described with the "super-atom" approach.[90] However, the lowest energy structures on the RSSR united-atom AMBER*/GBSA(water) and all-atom AMBER*/GBSA(water) surfaces were significantly different after 50 000 LM:MC steps and not in structural nor energetic agreement with the available experimental structures. Because of this, high level quantum calculations were performed in order to evaluate the other force fields available in the MacroModel program. The OPLSA-AA force field was found[95] to accurately reproduce the energetic and structural features of this system and was used for all subsequent conformational searches.

Conformational Search Results. The conformational flexibility of each of these systems was investigated using the LM:MC conformational search method (Table 2). Each search appears convergent with respect to the number of structures found, the energy of the lowest conformer and the number of times this structure is visited. Very few new structures are found after the first block of 5000 steps although each new block of searching begins at a new point on the potential energy surface. Further evidence of convergence was obtained by performing the same calculation on the *SRRS* enantiomer (data not shown), which resulted in the same ensemble as for the *RSSR* system. This suggests that the lowest energy structures found are, indeed, the global minima for each diastereomer (Figure 2) and that the generated ensembles are representative of the low energy structures of **1** on the OPLSAA/GBSA(water) surface.

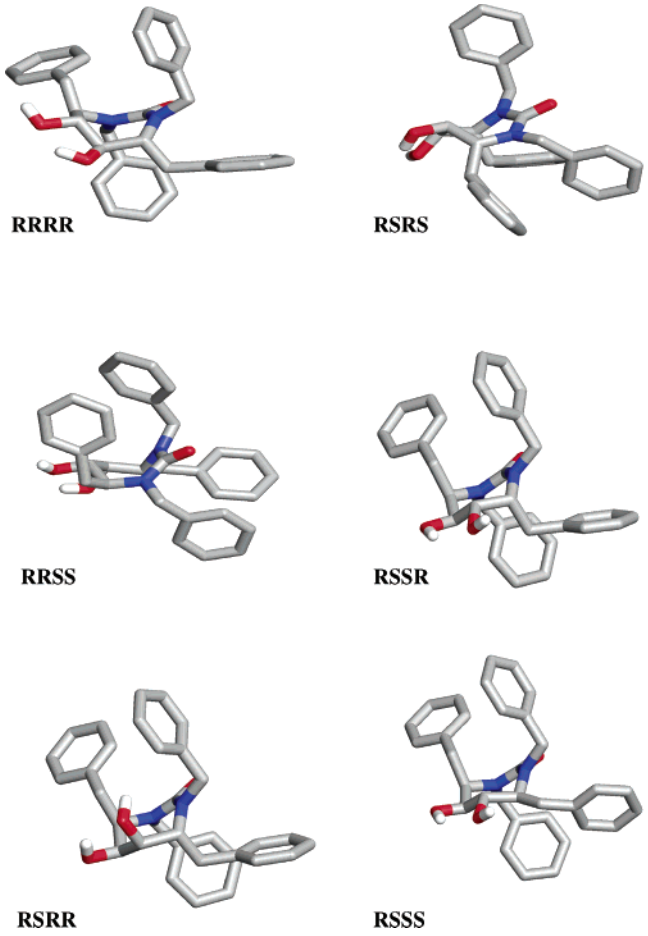

Figure 2. Lowest energy structures of the diastereomers of **1** found after 55 000 LM:MC search steps on the OPLSAA/GBSA(water) surface.

Analysis of the Diastereomeric Global Minima. The *RSSR* stereoisomer displays the highest experi-

Table 3. Comparison of Energetics for the Lowest Energy Diastereomers **1**[a]

structure	K_i (nM)	total *E*	*E* (str)	*E* (bnd)	*E* (tor)	*E* (o−p)	*E* (vdw)	*E* (elec)	solvation energy	GB energy	SA energy	ring conform.
RSSR	3.6	24.8	17.18	33.26	63.91	1.46	73.25	−104.19	−60.00	−78.51	18.52	chair
RSRR	6.0	46.0	16.59	36.92	80.00	1.82	69.15	−112.80	−46.56	−65.39	18.83	chair
RSRR	6.4	61.8	18.47	37.36	89.20	1.21	84.54	−108.13	−60.85	−79.64	18.79	chair
RSRS	250	66.4	22.86	61.66	54.67	1.44	99.30	−110.18	−63.39	−82.93	19.54	boat
RRRR	1350	54.6	17.46	26.21	109.79	0.87	84.12	−125.16	−58.69	−77.72	19.03	boat
RRSS	na	72.5	20.99	36.26	102.79	0.36	85.85	−118.11	−55.63	−73.41	17.78	boat

[a] All energy terms are in kJ mol^{-1}.

mental binding affinity for the HIV-1 protease[25] and is the most energetically favored of the cyclic urea isomers studied here (Tables 1 and 2). The least stable diastereomer is *RRSS*. This is the only diastereomer for which a synthesis was not successful. With the exception of the RRRR isomer, lower energy diastereomers tend to exhibit a higher experimental binding affinity. For instance, the *RSSR*, *RSRR* and *RSSS* are three of the four lowest energy diastereomers (the *RRRR* is the fourth) and they also show the strongest binding.

An examination of the various component energies for each diastereomer reveals that the greatest variability is in the torsional component (Table 3). *RSRS* is high in energy because of a large bending strain energy and unfavorable VDW interaction while *RRSS* is high in energy due to a large torsional strain energy. *RRRR* also possesses a large torsional energy: however, this is offset by the ability to adopt a conformation in which there is a larger than average stabilizing electrostatic energy. The large torsional strain energies in these systems are caused by the energetic preference for the boat conformation. *RSRR* is higher in energy than the other chair structures (*RSSR* and *RSRR*) due to rather small increases in destabilizing interactions (i.e. stretching, bending, torsional, van der Waals) along with a small decrease in stabilizing electrostatic interactions.

To interact with the protease, this diastereomeric series of inhibitors must be at least partially desolvated. The free energy associated with this process contributes to the overall binding free energy.[64] The GBSA energy has been previously shown[91] to be an accurate approximation for determining the free energy of solvation. With this in mind, the relative free energy of solvation of these diastereomers in the absence of the protease was estimated using the GBSA energies for each of the global minima shown in Figure 2. The GBSA method computes the free energy of solvation as

$$G_{sol} = G_{cav} + G_{vdw} + G_{pol}$$

where the solvent−solvent free energy of cavitation (G_{cav}) and the solute−solvent van der Waals interaction (G_{vdw}) are described using the solvent accessible surface area (SASA) and the free energy of polarization is described using a modification of the Generalized Born (GB) method. An analysis of the SASAs indicates that the shapes for these diastereomers are similar due to the rigid nature of the seven-member ring scaffold (ave. SASA = 733.1 Å^2; std. dev. = 23.0 Å^2). The smaller SASA for *RRSS* (693.0 Å^2) is due to a "tighter" arrangement of benzylic arms relative to the other global minima; in this structure each benzyl group is almost perfectly perpendicular to the plane of the ring and parallel with respect to its symmetrically equivalent benzylic partner. The ∼16 kJ mol^{-1} range in solvation free energies among these diastereomeric global minima is mainly due to variability in the GB polarization energy (Table 3). The least negative GB energy and hence the smallest favorable solvation energy occurs for the *RSRR* diastereomer; however, experimentally this structure is one of the tighter binders. The GBSA-based solvation free energy analysis predicts that *RSRR* is less soluble in bulk water but less energy is necessary to desolvate this diastereomer prior to binding with the protease. However, the SRSR enantiomer does not display a high binding affinity (Table 1) indicating that favorable desolvation energy is a necessary but not sufficient criterion for high binding affinity in this diastereomeric series. The most negative solvation energy corresponds to *RSRS*, and this diastereomer possesses one of the smallest binding affinities in the series. From this analysis, it is concluded that *RSSR*, *RSRR* and *RSRS* have the largest free energies of solvation, *RSRR* has the smallest free energies of solvation, and these energies of solvation show very little correlation with experimental binding affinity.

Crystal structures for *RSSR* cyclic urea inhibitors that are similar to **1** have been determined in the presence of the active site[8,18,20,21,26,27,30,33,36,37,39] and as the free ligand.[16,36,39] In addition, an NMR solution structure is available.[23] In all of these studies the *RSSR* inhibitor adopts a chair conformation in the presence and absence of the active site and in the liquid and solid phase, indicating that the system is preorganized for binding to the HIV protease. The global minimum energy structures shown in Figure 2 reveal that the isomers with highest binding affinities (*RSSR*, *RSRR* and *RSRR*) are in the chair conformation while those with much lower binding affinities (*RSRS*, *RRRR*, *RRSS*) occur in the boat conformation. Of course, in an achiral environment the enantiomeric partner to these tight binders (*RSSR*/*SRRS*, etc.) is also in the chair conformation. Therefore, a comparison of the binding affinities with the global minimum structures suggests that the ability to adopt a low energy chair conformation is a necessary but not sufficient requirement for binding. Each diastereomer is shown superimposed on the NMR ligand structure in Figure 3.

It has been hypothesized that substituents larger than hydrogens on the cyclic urea nitrogen atoms play an important role in the orientation of the ring substituents.[36] X-ray and solution NMR structures of the free and bound N,N′-substituted *RSSR* cyclic ureas indicate a preference for pseudodiaxial benzylic substituents and pseudodiequatorial hydroxyls. In the presence of the protease the hydroxyl groups point toward the floor of the active site and participate in hydrogen bonding with protease aspartic acids (Asp 25 and 25′). The P1/P1′ and

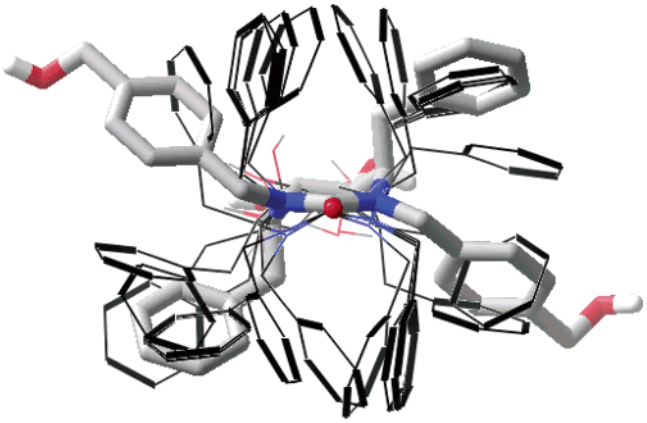

Figure 3. A superposition of the diastereomeric global minimum of **1** onto the NMR determined solution structure from 1bvg.pdf[92,93] (highlighted with polytube representation).

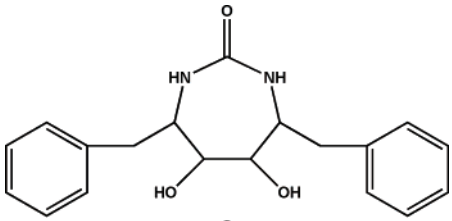

2

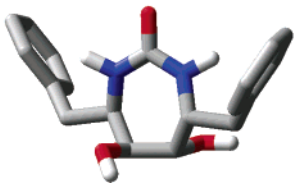

Figure 4. Top: N,N′-unsubstituted cyclic urea used to study the effects of 1,2-allylic and 1,3-axial strain. Bottom: OPLSAA/GBSA(water) global minimum energy structure.

P2/P2′ benzylic substituents are oriented in a pseudoaxial and pseudoequatorial manner, respectively, and interact with the hydrophobic S1/S1′ and S2/S2′ pockets of the enzyme. These conformational preferences have been explained by invoking dominant 1,2-allylic strain arguments for N,N′-substituted cyclic ureas such as **1** and dominant 1,3-diaxial strain arguments for N,N′-unsubstituted cyclic ureas such as for **2** (Figure 4). Ordinarily 1,3-diaxial strain would not allow both the hydroxyl and *N*-benzyl substituents to adopt an equatorial arrangement; however, when the N atoms are substituted as in **1**, the partial double bond character of the urea C−N bond results in a dominant 1,2-allylic strain. Hence, it would be predicted that the lowest energy structures of **1** would adopt conformations with pseudodiequatorial, pseudodiaxial and pseudodiequatorial orientations at the N(1,3), C(4,7) and C(5,6) atoms, respectively.[36] N, N′-*unsubstituted* cyclic ureas would adopt diaxial hydroxyl and diequatorial benzyl substituent orientations. Overall, the global minimum energy structures of **1** shown in Figure 2 are in general agreement with these strain arguments regardless of chirality.

Each diastereomeric global minimum of **1** contains pseudodiequatorial hydroxyl groups, except *RSRR* in which one hydroxyl is pseuodaxial. The P1/P1′ substituents are all pseudoaxial except *RRSS* and *RSRR* where one substituent in each is equatorial. In these global minima the P2 and P2′ substituents are pseudodiequatorial except for *RSRR* where one benzyl arm is pseudoaxial. The calculated global minima obey the 1,2-diaxial strain substituent rules with the following ring substituent orientations about the N1, C7, C6, C5, C4, N3 ring atoms: *RSSR*, *RSRS*, *RRRR* = eq/ax/eq/eq/ax/eq; *RSRR* = eq/ax/ax/eq/ax/eq; and *RSRR*, *RRSS* = eq/ax/eq/eq/eq/eq. It is clear that the inhibitor must align properly with the protease active site; however, all of the diastereomeric global minima are able to adopt conformations that are similar to the experimental ligand as shown in Figure 3. These results indicate that the binding affinities are dependent upon subtle differences in the P1/P1′ and P2/P2′ substituent orientation.

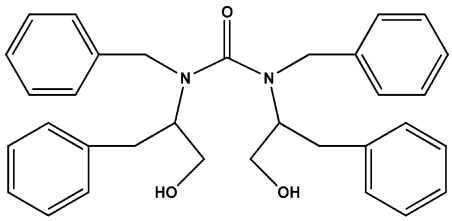

3

Figure 5. Acyclic seco urea compound used to study the importance of the cyclic urea ring scaffold.

We performed 55 000 LM:MC conformational search steps on the OPLSAA/GBSA(water) surface of the *RSSR* N,N′-unsubstituted **2** to evaluate the competing 1,2-allylic and 1,3-diaxial effects on the cyclic urea systems. This is a relatively rigid system; only fourteen low energy conformations are found within 25.0 kJ mol^{-1} of the lowest energy structure. The global minimum (Figure 4) contains diaxial hydroxyls and diequatorial benzyl substituents in agreement with the conformational hypothesis presented in the previous literature.[36] Of the fourteen low energy structures found in this study, nine are in the chair conformation with diaxial hydroxyls and diequatorial benzyl substituents. Of the five boat conformations, four contain structures with one hydroxyl in the equatorial position and all five contain structures with one axial and one equatorial benzylic substituent. The preponderance of low energy N,N′-unsubstituted *RSSR* cyclic urea conformations with diaxial hydroxyls in the solution phase explains why these systems show such poor binding affinity for the protease enzyme (experimental K_i = 4500 nM[16]). Significant reorganization would be necessary to optimally align the inhibitors with the active site.

The cyclic urea class of HIV inhibitors was designed with the help of a 3D pharmacophore that searched for molecular hits containing (1) intramolecular P1/P1′ substituent distances suitable for binding with the S1−S1′ protease hydrophobic pockets and (2) intramolecular distances between P1/P1′ substituents and hydrogen bond donor/acceptor substituents suitable for anchoring the inhibitor to the catalytic aspartates at the bottom of the active site.[41] The distances in each ensemble determined in this study were measured to see if the three-dimensional diastereomeric shape, as defined by the pharmacophore, could be correlated to binding affinity. The results indicate that all structures in all diastereomeric ensembles contained distances that matched the pharmacophore. Therefore, this evaluation

Table 4. Analysis of the Interactions between the HIV Protease (1bvg.pdf)[92,93] and the Diastereomeric Global Minimum Energy Structures Obtained after Manual Rigid-Body Docking[a]

	RSSR	*RSRR*	*RSRR*	*RSRS*	*RRRR*	*RRSS*
number of bad contacts:	65	76	68	81	80	105
nature of the bad contacts:						
substituent/residue:						
P2 /ILE 50	1	2	2	2	2	2
P2/ILE 84		1				1
P2/ILE 47			1		1	
P2/Val 32		1				
P1/ILE 47				1		1
P1/ILE 50				1	1	2
P1/ILE 84						1
P1/ALA28						1

[a] A "1" or a "2" indicates either one or both symmetrically equivalent residues make bad contacts with the inhibitor.

of diastereomeric shape does not correlate to the binding affinities. A schematic of the pharmacophore and a detailed analysis of the ability of the conformational ensembles to match the pharmacophore can be found in the Supporting Information.

Lam et al.[36] have obtained the HIV-1 binding affinities of the tetrabenzyl acyclic seco urea compound **3** (Figure 5) and compared them to the binding affinities of the cyclic *RSSR* diastereomer **1**. They found that the acyclic compound binds more than 2500 times less tightly, and they estimated that should the low energy conformers of **3** adopt mainly pseudocyclic rather than extended low energy conformations, then the contribution to the binding energy caused by preorganization of the side chains and diols should be approximately 4.8 kcal mol^{-1}.

A 55 000 LM:MC search on the OLPSAA/GBSA(water) surface (Table 4S in Supporting Information) was performed to determine the conformational preference of this system and to understand how the rigidity of the ring scaffold effected the conformational behavior. The resulting ensemble is dominated by extended conformations; i.e., only 129 of 655 structures within 25.0 kJ mol^{-1} of the lowest energy structure adopted pseudocyclic conformations that can be thought of as preorganized for binding to the protease active site. The first pseudocyclic structure appears 11.8 kJ mol^{-1} higher in energy than the lowest energy structure (Figure 6) and the remaining such structures are energetically scattered throughout the ensemble. From this it can be concluded that the seco system would have to undergo considerable reorganization in order to adopt a conformation that would optimally project the substituents into the protease hydrophobic pockets and align the hydroxyls with the catalytic aspartates.

To further ascertain the role of preorganization in this diastereomeric series, a rigid body docking of each global minimum structure with the HIV-1 protease was performed. The NMR solution phase protease−ligand complex[23] was utilized and each calculated diastereomeric global minima was superimposed onto the experimental ligand in the presence of the active site. The number of bad contacts[94] between each diastereomer and the HIV protease was determined (Table 4). *RSSR*, *RSRR* and *RSRR* contain fewer bad contacts than *RSRS*, *RRRR* and *RRSS*. In all systems the P2/P2′ benzyl arms make bad contacts with ILE 50 and ILE 50′ except for *RSSR* where only one such bad contact occurs. *RSRR* and *RSRR*, two of the better binding diastereomers, contain bad contacts between one of the P2 substituents and

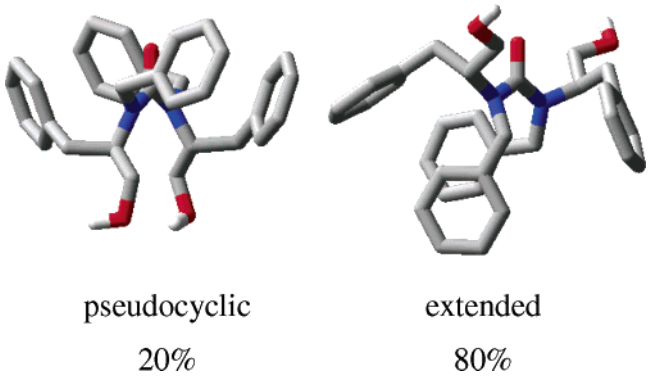

Figure 6. Representative pseudocyclic and extended conformations of **3** determined using the XCluster program (comparison atoms C2, N1 C7, C6, O10, N3, C4, C5, and O9 (see Figure 1 for atom numbers). Only 20% of the low energy structures found adopted the pseudocyclic conformation. The lowest energy structure belongs to the extended family represented by the structure on the right and the lowest energy pseudocylic conformer (11.8 kJ mol^{-1} higher in energy) belongs to the family represented by the structure on the left.

ILE 47 (*RSRR*) or ILE 84 (*RSRR*). Most notably, steric repulsions involving P1 and/or P1′ substituents occur in the *RSRS*, *RRRR* and *RRSS* diastereomers, and these are also the weaker binders. This analysis indicates that while all of the diastereomers are able to adopt conformations that are in general complementary to the active site, inhibitors with higher binding affinities are more precisely oriented for complementarity of fit with the protease active site. These results also indicate that less than optimal interaction with the P1/P1′ pockets plays a more important role in potency than interaction with the P2/P2′ pockets, which contradicts previously reported theoretical results.[70]

Analysis of the Diastereomeric Ensembles. It is interesting to compare the conformational behavior of all of the structures in each diastereomeric ensemble, as the number of low lying structures represents the flexible nature of the molecule. If every conformation is structurally distinct from all other conformations, then the number of unique minima provides quantitative information about the flexibility and the complexity of each potential energy surface. A larger number of unique minima indicate a more complex potential energy surface. The *RSSR* diastereomer contains eight low energy structures, and this is the smallest number of conformers found for any of the diastereomers, while the *RSRS* conformer contains 82 structures, the largest number. The *RSSR* diastereomer shows the highest

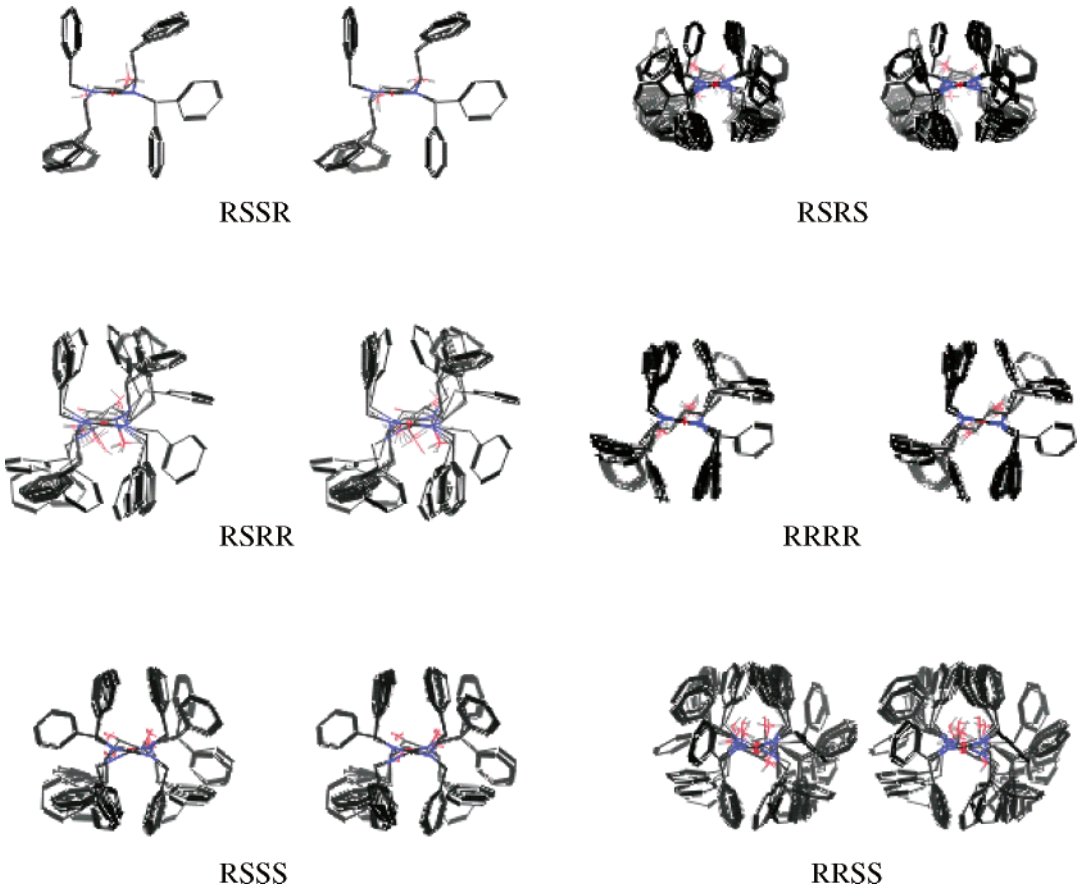

Figure 7. Stereoviews of the ensemble of structures for each diastereomer viewed down the C═O axis.

binding affinity for the HIV protease, while the *RSRS* diastereomer is ranked fourth in binding affinity (Table 1). Assuming other convergence criteria are satisfied, then the number of times the search revisits a particular structure is an indication of an exhaustive search. The *RSSR* diastereomer contains such a small number of unique minima that the lowest energy structure is revisited more than 5000 times near the end of the 55 000 step search. Searches on diastereomers with a larger number of minima revisit the lowest energy structure less often; however, even in these cases the search revisits the global minimum more than 300 times. Interestingly, the *RSRS* system contains the largest number of unique minima, yet the *RRRR* diastereomer with 19 unique minima is the system with the smallest number of lowest energy revisits. This indicates large regions of high energy on the PES. Since sampling of these regions does not lead to incorporation of more unique minima, the search becomes less efficient. According to the number of unique minima, the overall ordering of flexibility is *RSSR* < *RSRR* < *RRRR* < *RSRR* < *RRSS* < *RSRS*. However, it is possible that unique minima are not structurally distinct, i.e., that one or more structures can be grouped into conformationally similar families. When this occurs, the number of families is a better indicator of flexibility than the number of unique conformations. Therefore, the structures in each ensemble were examined in detail below.

All of the structures in each ensemble were superimposed using the seven ring atoms. Stereoviews of these superpositions are shown in Figure 7 and enable a visual examination of the number of unique structures and the differences in the flexibility of each ensemble. *RSSR* has the fewest while *RSRS* has the largest number of structures. *RRSS* has half the number of structures (42) as *RSRS* (82), yet the ensemble is more flexible, sweeping out more of the available conformational space. *RSRR* and *RRRR* contain a similar number of structures (18 and 19, respectively), yet the superpositions show that *RRRR* is clearly less flexible with respect to substituent orientation. From this analysis, the following rank order of flexibility is assigned: *RSSR* < *RRRR* < *RSRR* ~ *RSRR* < *RSRS* < *RRSS*.

To obtain an idea of the distribution of structures in each ensemble as well as to compare with an experimentally determined structure, the ring atoms of each of the 10 lowest energy structures of each ensemble were superimposed on the NMR structure of the cyclic urea ligand and the RMS deviation measured (Table 5). The low energy structures of the tightest binders (*RSSR*,

Table 5. Comparing Ensemble Structures with the NMR-Averaged Structure (1bvg.pdb) and the *RSSR* Global Minimum. Average[a] RMSD Values after Ring Atom Superimposition (N1−C7*−C6*−C5*−C4*−N3−C2)

comparison	average RMSD (Å) (1bvg.pdb)	average RMSD (Å) (*RSSR* global minimum)
RSSR	0.04	0.01
RSRR	0.07	0.05
RSRR	0.13	0.15
RRRR	0.44	0.44
RSRS	0.45	0.48
RRSS	0.51	0.54

[a] Average values determined for the 10 lowest energy structures (less if the ensemble contains fewer than 10 structures.)

Table 6. Ring Conformation and Substituent Orientation for the Calculated Ensembles of **1**

ensemble	number of structures	chair	boat	3a/4b/7b/1a[b]	3a/4b/7a/1b[b]	3b/4a/7a/1b[b]	3a/4a/7a/1a = 3b/4b/7b/1b[b]
RSSR	8	8	0	0	8	0	0
RSSR (ref 16[a])	14	14	0	0	14	0	0
RSRR	18	12	6	1	17	0	0
RSRR	28	19	9	12	16	0	0
RSRS	82	9	73	22	10	11	37
RRRR	19	0	19	1	18	0	0
RRSS	45	14	31	11	33	0	0

[a] Similar structure to *RSSR*, energy window ~21 kJ mol^{-1}. [b] Orientation relative to the plane of the ring; a = above, b = below.

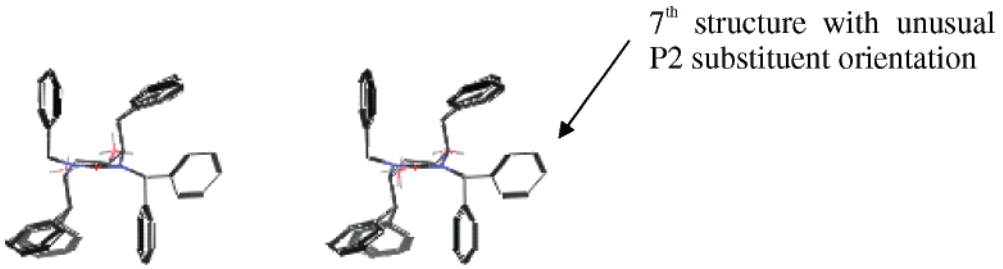

Figure 8. Stereoview of the eight structures in the *RSSR* ensemble superimposed according to ring atom alignment.

RSRR and *RSRR*) are most structurally similar to the NMR averaged structure, indicating that the shape and flexibility of the diastereomers plays an important role in binding. The best binders are less flexible, as indicated by the smaller number of low energy structures on their PES. They are also in the "proper" shape or orientation for optimal interaction with the protease active site as indicated by the small RMS deviation from the experimental structure. For instance, the *RRRR* diastereomer is relatively rigid; however, with an ensemble made up entirely of boat conformations, it is not able to preorganize in solvent for optimal binding with the active site. Further characterization of the structures was obtained by superimposing the global minimum for *RSSR* with the 10 lowest energy structures from each of the other diastereomeric ensembles (Table 5). The *RSSR* global minimum was chosen as it was the most representative of its corresponding ensemble, and it had the smallest RMS deviation from the crystal structure ligand. This analysis confirms that diastereomers with low binding affinities deviate significantly from the solution phase behavior of the *RSSR* diastereomer while high binding affinity diastereomers are structurally very similar to the *RSSR* ensemble.

Most of the experimentally determined cyclic urea structures are oriented with the benzyl substituents arranged in a propeller-like arrangement, with alternation above and below the plane of the ring, and this facilitates alignment with the hydrophobic enzyme pockets.[16] Table 6 provides detailed information on the shape of the rings and the substituent orientation for each diastereomeric ensemble calculated in this study. All of the calculated *RSSR* low energy structures adopt conformations in agreement with experimentally observed structures as do more than 94% of the *RSRR* conformations. Other diastereomers contain increasing numbers of low energy structures that differ from the experimental ligand shape. For instance, only 12% of the low energy *RSRS* structures agree with the observed conformational preferences for a propeller-like arrangement of benzyl substituents, and more than 45% of the structures are oriented with all four benzyl arms on one side of the ring plane, prohibiting alignment with the active site.

Clustering the minima into conformational families yields further information about molecular flexibility. The XCluster program was used to determine if the ensembles naturally form structurally related groupings and if the groupings are the same or different for each ensemble. Clustering by atomic RMS after rigid body superposition of all heavy atoms did not lead to significant clustering in any of the ensembles as evidenced by distance maps, mosaics and separation ratios. Clustering the ensembles with respect to ring conformation, using a superposition of ring atoms N1−C7*−C6*−C5*−C4*−N3−C2 (Figure 1), resulted in very strong clustering in most cases as described below.

***RSSR* Ensemble (experimental K_i = 3.6 nM).** Only eight minima were found within 25 kJ mol^{-1} of the lowest energy structure on the OPLSAA/GBSA(water) surface (Figures 7 and 8). These structures are all in the chair conformation with very similar substituent orientations. The average RMSD between the ring atoms in structures 2−8 and in the global minimum is 0.01 Å. The structures differ mainly in the orientation of the hydroxyl groups with some variability in one of the P2 benzyl arms. One structure that lies 23.43 kJ mol^{-1} above the global minimum is significantly different from the others; in this conformer one of the P2 substituents is bent up above the plane rather than pointing down below the plane of the ring (Figure 8). This creates a larger distance between the P1 and P2 substituents (6.4 Å vs 5.0 Å average; 4.8 Å to 5.3 Å range of distances in structures 2−8.) The global minimum energy structure is relatively representative of the structures in the ensemble.

***RSRR* Ensemble (experimental K_i = 6.0 nM).** Eighteen minima were found within 25 kJ mol^{-1} of the lowest energy structure on the OPLSAA/GBSA(water) surface (Figures 7 and 9). There is significant variability in these structures with respect to ring conformation and substituent orientation. The ensemble contains twelve chair and six boat conformations. The orientation of P2/P2′ benzyl arms is relatively conserved while the

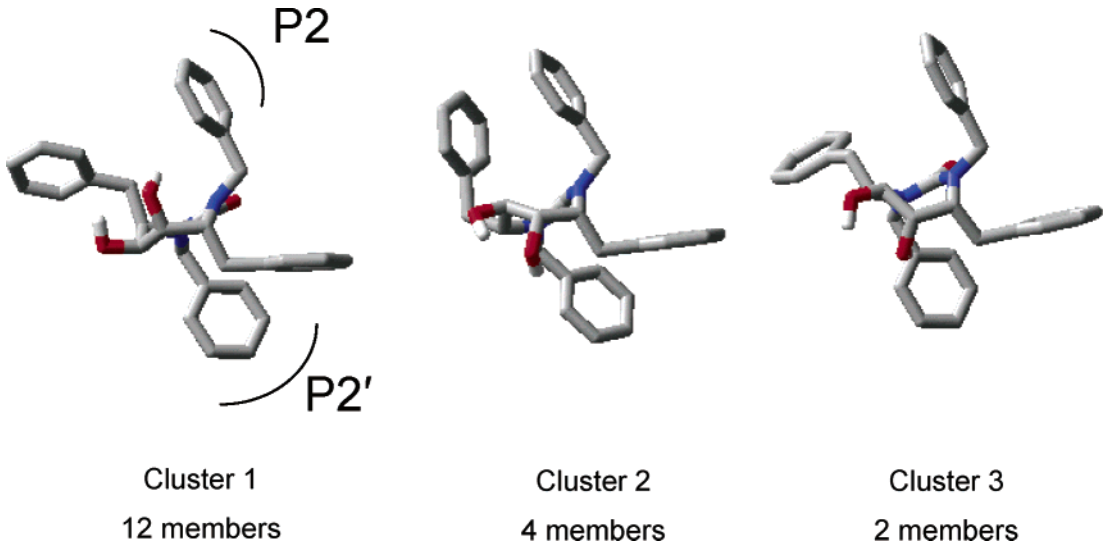

Figure 9. Representative structures of the three conformational families of *RSRR*.

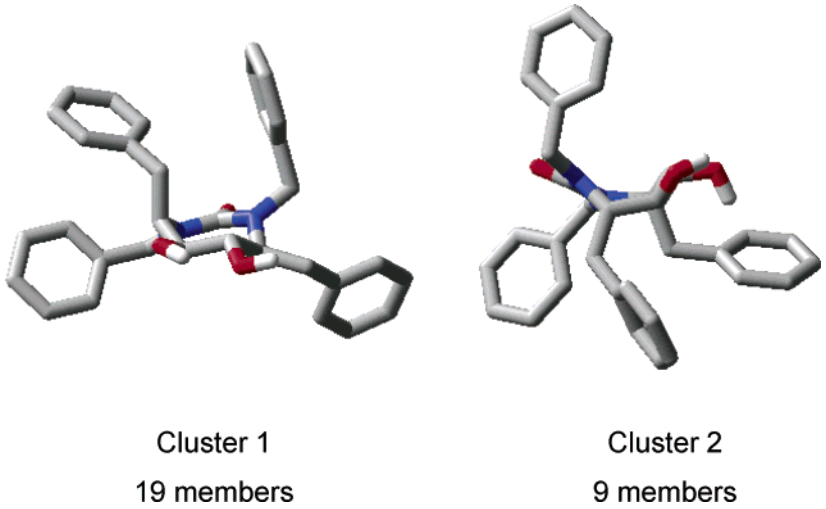

Figure 10. Representative structures of the two conformational families of *RSRR*.

position of the P1/P1′ substituents is highly variable. The hydroxyl orientations are much more variable than in the *RSSR* ensemble. The global minimum structure is not representative of the ensemble behavior. The ensemble can be clustered into three conformational families with distinctly different representative structures (separation ratio = 6.4 to 18.5; see Figure 12). The largest difference between these families is in the ring conformation, the orientation of the hydroxyl groups, and one of the P1 benzyl arms. The first cluster is the largest with twelve members and contains chair conformers with pseudoequatorial P2/P2′ substituents, pseudoaxial P1/P1′ substituents, and one pseudoaxial and one pseudoequatorial hydroxyl group. The second cluster contains four boat conformers with pseudodiequatorial hydroxyls and one pseudoequatorial P1 substituent. The third cluster contains two boat conformations with pseudoaxial and pseudoequatorial hydroxyls.

***RSSS* Ensemble (experimental K_i = 6.4 nM).** Twenty-eight structures were found within 25 kJ mol^{-1} of the lowest energy structure with nineteen structures adopting the chair and nine structures adopting the boat conformation. Similar variability in the substituent orientations is found as for the *RSRR* diastereomer; however, the diequatorial hydroxyl orientation is more highly conserved. The global minimum structure is not very representative. The ensemble can be strongly clustered (separation ratio = 18.6) into two conformational families with distinctly different representative structures that can be distinguished by their boat versus chair conformations (Figure 10).

***RSRS* Ensemble (experimental K_i = 250 nM).** The most structures (82) were found on this surface with the largest number of boat conformations (73). The global minimum is a boat with the first chair appearing 8.9 kJ mol^{-1} higher in energy. In the ensemble of structures, the hydroxyl orientations are highly variable and the substituents sweep out a large part of the conformational space available to them (Figure 7). The P2/P2′ and one of the P1 substituents tend to vary their orientation above and below the plane of the ring. The other P1 substituent orientation is relatively conserved. The global minimum structure is not very representative; however, the ensemble can be strongly clustered (separation ratio = 6.2−6.7) into three conformational families with distinctly different representative structures (Figure 11).

***RRRR* Ensemble (experimental K_i = 1350 nM).** Nineteen structures were found for this system. The global minimum is a boat and no chair conformations

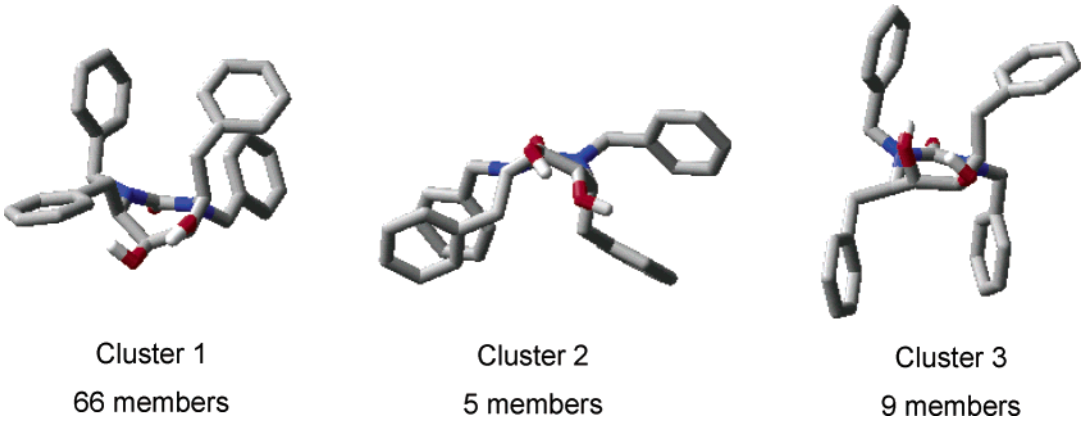

Figure 11. Representative structures of the three conformational families of *RSRS*.

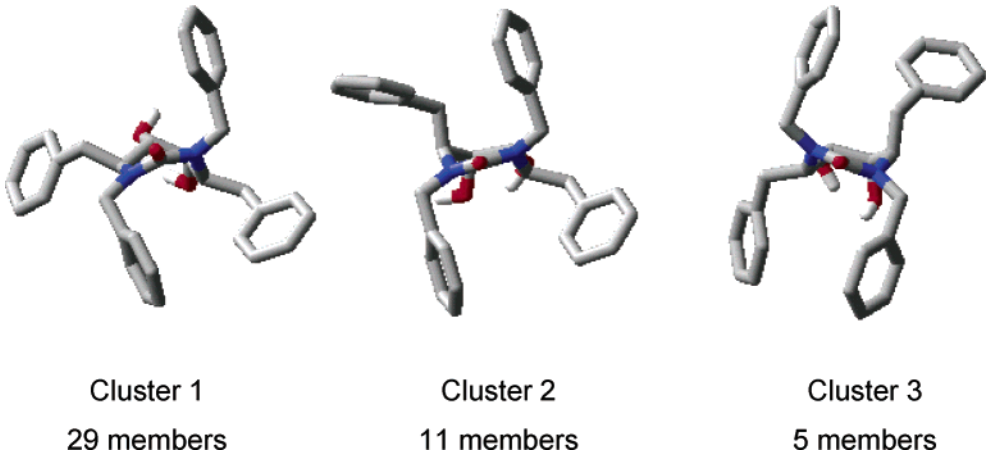

Figure 12. Representative structures of the three conformational families of *RRSS*.

are found within 25.0 kJ mol^{-1}. This is a highly conserved ensemble; i.e., the ring atoms all superimpose cleanly and the P2/P2′ orientations are conserved. There is small variability in the P1/P1′ orientations although far less than in most other diastereomeric ensembles. The global minimum structure is representative of the ensemble.

***RRSS* Ensemble (experimental K_i = na).** This is the second largest ensemble with 45 structures. This is also the most flexible structure as shown by the stereoview of the ensemble superposition (Figure 7). The ring atoms are not conserved, the hydroxyls adopt many different orientations, and the benzyl arms sweep out a considerable amount of space and randomly orient above and below the plane of the ring. The global minimum is a boat with the first chair appearing 2.3 kJ mol^{-1} higher in energy. The ensemble contains 14 chair and 31 boat conformations. The global minimum structure is not very representative. The ensemble can be strongly clustered (separation ratio = 7.0−8.6) into three conformational families with distinctly different representative structures (Figure 12).

Conclusions

The Low Mode:Monte Carlo conformational search method has been shown capable of exhaustively searching the OPLSAA/GBSA(water) surface and was used to identify the ensemble of all low lying structures of a series of diastereomeric cyclic urea HIV protease inhibitors. An energetic analysis indicates that there is a good correlation between the OPLSAA/GBSAA(water) energies (enthalpies) and the different binding affinities of each stereoisomer. A detailed examination of each ensemble indicates that inhibitors with higher binding affinities are generally more rigid and in the proper shape for optimal interaction with the protease active site. In addition, the ability to adopt a chair conformation encourages ring substituents to adopt optimal binding orientations. An analysis of the solvation free energy, as approximated by the GBSA energies, does not correlate to binding affinity. A comparison with the conformational preferences of N,N-unsubstituted cyclic ureas indicates that N substitution plays an important role in orienting the substituents for optimal interaction with the active site. The N,N-substituted cyclic ureas studied here are all able to adopt conformations that are in general complementary to the protease active site; however, a rigid body docking experiment indicated that inhibitors with higher binding affinities (*RSSR*, *RSRR* and *RSRR*) are more precisely oriented for optimal interaction than are inhibitors with low binding affinities (*RSRS*, *RRRR* and *RRSS*). Therefore, binding affinities are dependent upon subtle differences in the P1/P1′ and P2/P2′ substituent orientation.

Acknowledgment. Acknowledgment is made to the donors of the Petroleum Research Fund, administered by the American Chemical Society, for partial support of this research. Undergraduate summer research stipends were also provided by grants from the Merck Foundation administered by the American Association for the Advancement of Science, the Patchett Family

Foundation, and the Council on Undergraduate Research. Computational resources were provided in part by the MERCURY supercomputer consortium (http://mars.hamilton.edu) under NSF grant CHE-0116435. Last, we are grateful to have received support from the Hobart and William Smith Colleges Faculty Research Program.

Supporting Information Available: A comparison of the conformational ensembles of **1** with a previously reported pharmacophore model along with the conformational search results for the acyclic seco-form of **1.** are available as supplemental information. This material is available free of charge via the Internet at http://pubs.acs.org.

References

(1) Hodge, C. N.; Straatsma, T. P.; McCammon, J. A.; Wlodawer, A. Rational Design of HIV Protease Inhibitors. *Structural Biology of Viruses*; Chiu, W., Burnett, R. M., Garcea, R. L., Eds.; Oxford University Press: New York, 1997; pp 451−473.

(2) Appelt, K. Crystal Structures of HIV-1 Protease-Inhibitor Complexes. *Perspect. Drug Discovery Des.* **1993**, *1*, 23−48.

(3) Wlodawer, A.; Erickson, J. W. Structure-Based Inhibitors of HIV-1 Protease. *Annu. Rev. Biochem.* **1993**, *62*, 543−585.

(4) Brik, A.; Wong, C.-H. HIV-1 Protease: Mechanisms and Drug Discovery. *Org. Biomol. Chem.* **2003**, *1*, 5−14.

(5) Wlodawer, A. Rational Approach to AIDS Drug Design through Structural Biology. *Annu. Rev. Med.* **2002**, *53*, 595−614.

(6) Tomasselli, A. G.; Heinrikson, R. L. Targeting the HIV−Protease in AIDS Therapy: A Current Clinical Perspective. *Biochim. Biophys. Acta* **2000**, *1477*, 189−214.

(7) Eron, J. J. J. HIV-1 Protease Inhibitors. *Clin. Infect. Dis.* **2000**, *30*, 160−170.

(8) Ala, P. J.; Huston, E. E.; Klabe, R. M.; McCabe, D. D.; Duke, J. L.; Rizzo, C. J. Molecular Basis of HIV-1 Protease Drug Resistance: Structural Analysis of Mutant Protease Complexed with Cyclic Urea Inhibitors. *Biochemistry* **1997**, *36*, 1573−1580.

(9) Hoegl, L.; Korting, H. C.; Klebe, G. Inhibitors of Aspartic Proteases in Human Diseases: Molecular Modeling Comes of Age. *Pharmazie* **1999**, *54*, 319−329.

(10) Wlodawer, A.; Vondrasek, J. Inhibitors of HIV-1 Protease: A Major Success of Structure-Based Drug Design. *Annu. Rev. Biophys. Biomol. Struct.* **1998**, *27*, 249−284.

(11) Ren, S.; Lien, E. J. Development of HIV Protease Inhibitors: A Survey. *Progress in Drug Research*; Jucker, E., Ed.; Birkhauser Verlag AG: Basel, 1998; pp 4−28.

(12) Flexner, C. HIV−Protease Inhibitors. *New Engl. J. Med.* **1998**, *338*, 1281−1292.

(13) Moore, J. P.; Stevenson, M. New Targets for Inhibitors of HIV-1 Replication. *Nat. Rev. Mol. Cell. Biol.* **2000**, *1*, 40−49.

(14) De Clercq, E. New Developments in Anti-HIV Chemotherapy. *Curr. Med. Chem.* **2001**, *8*, 1543−1572.

(15) De Clercq, E. New Developments in Anti-HIV Chemotherapy. *Pure Appl. Chem.* **2001**, *73*, 55−66.

(16) Hodge, C. N.; Lam, P. Y. S.; Eyermann, C. J.; Jadhav, P. K.; Ru, Y.; Fernandez, C. H.; De Lucca, G. V.; Chang, C.-H.; Kaltenbach, R. F.; Holler, E. R.; Woerner, F.; Daneker, W. F.; Emmett, G.; Calabrese, J. C.; Aldrich, P. E. Calculated and Experimental Low-Energy Conformations of Cyclic Urea HIV Protease Inhibitors. *J. Am. Chem. Soc.* **1998**, *120*, 4570−4581.

(17) Eyermann, C. J.; Jadhav, P. K.; Hodge, C. N.; Chang, C.-H.; Rodgers, J. D.; Lam, P. Y. S. The Role of Computer-Aided and Structure-Based Design Techniques in the Discovery and Optimization of Cyclic Urea Inibitors of HIV Protease. *Advances in Amino Acid Mimetics and Peptidomimetics*; Abell, A. D.; Elsevier Science Ltd.: New York, 1997; pp 1−40.

(18) Jadhav, P. K.; ala, P.; Woerner, F. J.; Chang, C.-H.; Garber, S. S.; Anton, E. D.; Bacheler, L. T. Cyclic Urea Amides: HIV-1 Protease Inhibitors with Low Nanomolar Potency against Both Wild-Type and Protease Inhibitor Resistant Mutants of HIV. *J. Med. Chem.* **1997**, *40*, 181−191.

(19) Wilkerson, W. W.; Dax, S.; Cheatham, W. W. Nonsymmetrically Substituted Cyclic Urea HIV Protease Inhibitors. *J. Med. Chem.* **1997**, *40*, 4079−4088.

(20) Nugiel, D. A.; Jacobs, K.; Worley, T.; Patel, M.; III, R. F. K.; Meyer, D. T. Preparation and Structure−Activity Relationship of Novel P1/P1′-Substituted Cyclic Urea-Based Human Immunodeficiency Virus Type-1 Protease Inhibitors. *J. Med. Chem.* **1996**, *39*, 2156−2169.

(21) Sham, H. L.; Zhao, C.; Stewart, K. D.; Betebenner, D. A.; Lin, S.; Park, C. H. A Novel, Picomolar Inhibitor of Human Immunodeficiency Virus Type 1 Protease. *J. Med. Chem.* **1996**, *39*, 382−397.

(22) Wilkerson, W. W.; Akamike, E.; Cheatham, W. W.; Hollis, A. Y.; Collins, R. D.; DeLucca, I. HIV Protease Inhibitory Bis-Benzamide Cyclic Ureas: A Quantitative Structure−Activity Relationship Analysis. *J. Med. Chem.* **1996**, *39*, 4299−4312.

(23) Yamazaki, T.; Nicholson, L. K.; Torchia, D. A.; Wingfield, P.; Stahl, S. J.; Kaufman, J. D. NMR and X-ray Evidence That the HIV Protease Catalytic Aspartyl Groups Are Protonated in the Complex Formed by the Protease and a Non-Peptide Cyclic Urea-Based Inhibitor. *J. Am. Chem. Soc.* **1994**, *116*, 10791−10792.

(24) Kaltenbach, R. F. I.; Klabe, R. M.; Cordova, B. C.; Seitz, S. P. Increased Antiviral Activity of Cyclic Urea HIV Protease Inhibitors by Modifying the P1/P1′ Substituents. *Bioorg. Med. Chem. Lett.* **1999**, *9*, 2259−2262.

(25) Kaltenbach, R. F. I.; Nugiel, D. A.; Lam, P. Y. S.; Klabe, R. M.; Seitz, S. P. Stereoisomers of Cyclic Urea HIV-1 Protease Inhibitors: Synthesis and Binding Affinities. *J. Med. Chem.* **1998**, *41*, 5113−5117.

(26) Rodgers, J. D.; Johnson, B. L.; Wang, H.; Erickson-Viitanen, S.; Klabe, R. M.; Bacheler, L.; Cordova, B. C.; Chang, C.-H. Potent Cyclic Urea Hiv Protease Inhibitors with 3-Aminoindazole P2/P2′ Groups. *Bioorg. Med. Chem. Lett.* **1998**, *8*, 715−720.

(27) Rodgers, J. D.; Lam, P. Y.; Johnson, B. L.; Wang, H.; Ko, S. S.; Seitz, S. P. Design and Selection of DMP 850 and DMP 851: The Next Generation of Cyclic Urea HIV Protease Inhibitors. *Chem. Biol.* **1998**, *5*, 597−608.

(28) Patel, M.; Kaltenbach, R. F.; Nugiel, D. A.; McHugh, R. J.; Jadhav, P. K.; Bacheler, L.; Cordova, B. C.; Klabe, R. M.; Erickson-Viitanen, S.; Garber, S.; Reid, C.; Seitz, S. P. The Synthesis of Symmetrical and Unsymmetrical P1/P1′ Cyclic Ureas as HIV Protease Inhibitors. *Bioorg. Med. Chem. Lett.* **1998**, *8*, 1977−1082.

(29) Patel, M.; Lee, T. B.; Rayner, M. M.; Cordova, B. C.; Klabe, R. M.; Erickson-Viitanen, S. The Synthesis and Evaluation of Cyclic Ureas as HIV Protease Inhibitors: Modifications of the P1/P1′ Residues. *Bioorg. Med. Chem. Lett.* **1998**, *8*, 823−828.

(30) Han, Q.; Chang, C.-H.; Li, R.; Ru, Y.; Jadhav, P. K.; Lam, P. Y. S. Cyclic HIV Protease Inhibitors: Design and Synthesis of Orally Bioavailable, Pyrazole P2/P2′ Cyclic Ureas with Improved Potency. *J. Med. Chem.* **1998**, *41*, 2019−2028.

(31) De Lucca, G. V.; Lam, P. Y. S. De Novo Design, Discovery and Development of Cyclic Urea HIV Protease Inhibitors. *Drugs Future* **1998**, *23*, 987−994.

(32) De Lucca, G. V.; Kim, U. T.; Liang, J.; Cordova, B. C.; Klabe, R. M.; Garber, S.; Bacheler, L.; Lam, G. N.; Wright, M. R.; Logue, K. A.; Erickson-Viitanen, S.; Ko, S. S.; Trainor, G. L. Nonsymmetric P2/P2′ Cyclic Urea Hiv Protease Inhibitors: Structure−Activity Relationship, Bioavailability, and Resistance Profile of Monoindazole-Substituted P2 Analogues. *J. Med. Chem.* **1998**, *41*, 2411−2423.

(33) Ala, P. J.; Huston, E. E.; Klabe, R. M.; Jadhav, P. K.; Lam, P. Y. S.; Chang, C.-H. Counteracting HIV-1 Protease Drug Resistance: Structural Analysis of Mutant Proteases Complexed with XV638 and SD146, Cyclic Urea Amides with Broad Specificities. *Biochemistry* **1998**, *37*, 15042−15049.

(34) Hultén, J.; Bonham, N. M.; Nillroth, U.; Hansson, T.; Zuccarello, G.; Bouzide, A. Cyclic HIV-1 Protease Inhibitors Derived from Mannitol: Synthesis, Inhibitory Potencies, and Computational Predictions of Binding Affinities. *J. Med. Chem.* **1997**, *40*, 885−897.

(35) Bäckbro, K.; Löwgren, S.; Österlund, K.; atepo, J.; Unge, T. Unexpected Binding Mode of a Cyclic Sulfamide HIV-1 Protease Inhibitor. *J. Med. Chem.* **1997**, *40*, 898−902.

(36) Lam, P. Y. S.; Ru, Y.; Jadhav, P. K.; Aldrich, P. E.; De Lucca, G. V.; Eyermann, C. J.; Chang, C.-H.; Emmett, G.; Holler, E. R.; Daneker, W. F.; Li, L.; Confalone, P. N.; McHugh, R. J.; Han, Q.; Li, R.; Markwalder, J. A.; Seitz, S. P.; Sharpe, T. R.; Bacheler, L. T.; Rayner, M. M.; Klabe, R. M.; Shum, L.; Winslow, D. L.; Kornhauser, D. M.; Jackson, D. A.; Erickson-Viitanen, S.; Hodge, C. N. Cyclic HIV Protease Inhibitors: Synthesis, Conformational Analysis, P2/P2′ Structure−Activity Relationshop, and Molecular Recognition of Cyclic Ureas. *J. Med. Chem.* **1996**, *39*, 3514−3525.

(37) Hodge, C. N.; Aldrich, P. E.; Bacheler, L. T.; Chang, C.-H.; Eyermann, C. J.; Garber, S. Improved Cyclic Urea Inhibitors of the HIV-1 Protease: Synthesis, Potency, Resistance Profile, Human Pharmacokinetics and X-ray Crystal Structure of DMP 450. *Chem. Biol.* **1996**, *3*, 301−314.

(38) Hultén, J.; Andersson, H. O.; Schaal, W.; Danielson, H. U.; Classon, B.; Kvarnström, I. Inhibitors of the C2−Symmetric HIV-1 Protease: Nonsymmetric Binding of a Symmetric Cyclic Sulfamide with Ketoxime Groups in the P2/P2′ Side Chains. *J. Med. Chem.* **1999**, *42*, 4054−4061.

(39) Ala, P. J.; DeLoskey, R. J.; Huston, E. E.; Jadhav, P. K.; Lam, P. Y. S.; Eyermann, C. J.; Hodge, C. N.; Schadt, M. C.; Lewandowski, F. A.; Weber, P. C.; McCabe, D. D.; Duke, J. L.; Chang, C.-H. Molecular Recognition of Cyclic Urea HIV-1 Protease Inhibitors. *J. Biol. Chem.* **1998**, *273*, 12325−12331.

(40) Kaltenbach, R. F.; Patel, M.; Waltermire, R. E.; Harris, G. D.; Stone, B. R. P.; Klabe, R. M.; Garber, S.; Bacheler, L.; Cordova, B. C.; Logue, K. A.; Wright, M. R.; Erickson-Viitanen, S.; Trainor, G. L. Synthesis, Antiviral Activity and Pharmacokinetics of P1/P1′ Substituted 3-Aminoindazole Cyclic Urea HIV Protease Inhibitors. *Bioorg. Med. Chem. Lett.* **2003**, *13*, 605−608.

(41) Lam, P. Y. S.; Jadhav, P. K.; Eyermann, C. J.; Hodge, C. N.; Ru, Y.; Bacheler, L.; Meek, J. L.; Otto, M. J.; Rayner, M. M.; Wong, Y. N.; Chang, C.-H.; Weber, P. C.; Jackson, D. A.; Sharpe, T. R.; Erickson-Viitanen, S. Rational Design of Potent, Bioavailable, Nonpeptide Cyclic Ureas as HIV Protease Inhibitors. *Science* **1994**, *263*, 380−384.

(42) Leach, A. R. *Molecular Modeling Principles and Applications*; 2nd ed.; Prentice Hall, Pearson Education: Harlow, England, 2001.

(43) Senderowitz, H.; Parish, C.; Still, W. C. Carbohydrates: United Atom AMBER* Parametrization of Pyranoses and Simulations Yielding Anomeric Free Energies. *J. Am. Chem. Soc.* **1996**, *118*, 2078−2086.

(44) Saunders: M.; Houk, K. N.; Wu, Y.-D.; Still, W. C.; Lipton, M.; Chang, G.; Guida, W. C. Conformations of Cycloheptadecane. A Comparison of Methods for Conformational Searching. *J. Am. Chem. Soc.* **1990**, *112*, 1419−1427.

(45) Weiner, P. K.; Profeta, S.; Wipff, G.; Havel, T.; Kuntz, I. D.; Langridge, R.; Kollman, P. A. A Distance Geometry Study of Ring Systems. Application to Cyclooctane, 18-Crown-6, Cyclododecane and Androstanedione. *Tetrahedron* **1983**, *38*, 1113.

(46) Crippen, G. M.; Havel, T. F. *Distance Geometry and Molecular Conformation*; John Wiley: New York, 1988.

(47) Havel, T. F. An Evaluation of Computational Strategies for Use in the Determination of Protein Structure from Distance Constraints Obtained by Nuclear Magnetic Resonance. *Prog. Biophys. Mol. Biol.* **1991**, *56*, 43.

(48) Peishoff, C. E.; Dixon, J. S. Improvements to the Distance Geometry Algorithm for Conformational Sampling of Cyclic Structures. *J. Comput. Chem.* **1992**, *13*, 565.

(49) Crippen, G. M. Exploring the Conformation Space of Cycloalkanes by Linearized Embedding. *J. Comput. Chem.* **1992**, *13*, 351.

(50) Fine, R. M.; Wang, H.; Shenkin, P. S.; Yarmush, D. L.; Levinthal, C. Predicting Antibody Hypervariable Loop Conformations. Minimization and Molecular Dynamics Studies of MCPC603 from Many Randomly Generated Loop Conformations". *Proteins: Struct., Funct., Genet.* **1986**, *1*, 342.

(51) Shenkin, P. S.; Yarmush, D. L.; Fine, R. M.; Wang, H.; Levinthal, C. Predicting Antibody Hypervariable Loop Conformation. Ensembles of Random Conformations for Ring-Like Structures. *Biopolymers* **1987**, *26*, 2053.

(52) Chang, G.; Guida, W. C.; Still, W. C. An Internal Coordinate Monte Carlo Method for Searching Conformational Space. *J. Am. Chem. Soc.* **1989**, *111*, 4379−4386.

(53) Weinberg, N.; Wolfe, S. A Comprehensive Approach to the Conformational Analysis of Cyclic Compounds. *J. Am. Chem. Soc.* **1994**, *116*, 9860−9868.

(54) Li, Z.; Scheraga, H. A. Monte Carlo-Minimization Approach to the Multiple-Minima Problem in Protein Folding. *Proc. Natl. Acad. Sci. U.S.A.* **1987**, *84*, 6611−6615.

(55) Freyberg, B. v.; Braun, W. Efficient Search for All Low Energy Conformations of Met-Enkephalin by Monte Carlo Methods. *J. Comput. Chem.* **1991**, *12*, 1065.

(56) Kolossvary, I.; Guida, W. C. Low Mode Search. An Efficient, Automated Computational Method for Conformational Analysis: Application to Cyclic and Acyclic Alkanes and Cyclic Peptides. *J. Am. Chem. Soc.* **1996**, *118*, 5011−5019.

(57) Kolossvary, I.; Guida, W. C. Low-Mode Confomational Search Elucidated: Application to C39h80 and Flexible Docking of 9-Deazaguanine Inhibitors into PNP. *J. Comput. Chem.* **1999**, *20*, 1671−1684.

(58) Kolossvary, I.; Keseru, G. Hessian-Free Low-Mode Conformational Search for Large-Scale Protein Loop Optimization: Application to C-Jun N−Terminal Kinase JNK3. *J. Comput. Chem.* **2001**, *22*, 21−30.

(59) Leach, A. R. A Survey of Methods for Searching the Conformational Space of Small and Medium-Size Molecules. *Rev. Comput. Chem.*; Boyd, K. B. L. a. D. B.; Wiley-VCH: New York, 1991; pp 1−55.

(60) Becker, O. *Computational Biochemistry and Biophysics*; Marcel Decker AG: New York, 2001; 69−90.

(61) Goodman, J. M. *Chemical Applications of Molecular Modeling*; Royal Society of Chemistry: Cambridge, 1998.

(62) Mohamadi, F.; Richards, N. G. J.; Guida, W. C.; Liskamp, R.; Lipton, M.; Caufield, C.; Chang, G.; Hendrickson, T.; Still, W. C. Macromodel − an Integrated Software System for Modeling Organic and Bioorganic Molecules Using Molecular Mechanics. *J. Comput. Chem.* **1990**, *11*, 440−467.

(63) Parish, C.; Lombardi, R.; Sinclair, K.; Smith, E.; Goldberg, A.; Rappleye, M.; Dure, M. A Comparison of the Low Mode and Monte Carlo Conformational Search Methods. *J. Mol. Graph. Mod.* **2002**, *21*, 129−150.

(64) Luque, F. J.; Barril, X.; Orozco, M. Fractional Description of Free Energies of Solvation. *J. Comput.-Aided Mol. Des.* **1999**, *13*, 139−152.

(65) Mardis, K. L.; Luo, R.; Gilson, M. K. Interpreting Trends in the Binding of Cyclic Ureas to HIV-1 Protease. *J. Mol. Biol.* **2001**, *309*, 507−517.

(66) Trylska, J.; Antosiewicz, J.; Geller, M.; Hodge, C. N.; Klabe, R. M.; Head, M. S.; Gilson, M. K. Thermodynamic Linkage between the Binding of Protons and Inhibitors to HIV-1 Protease. *Protein Sci.* **1999**, *8*, 180−195.

(67) Schaal, W.; Karlsson, A.; Ahlsen, G.; Lindberg, J.; Anderson, H. O.; Danielson, H. U.; Classon, B.; Unge, T.; Samuelsson, B.; Hulten, J.; Hallberg, A.; Karlen, A. Synthesis and Comparative Molecular Field Analysis (CoMFA) of Symmetric and Nonsymmetric Cyclic Sulfamide HIV-1 Protease Inhibitors. *J. Med. Chem.* **2001**, *44*, 155−169.

(68) Kotamarthi, B. Computational Design of New Cyclic Urea Inhibitors for Improved Binding of HIV-1 Aspartic Protease. *Biochem. Biophys. Res. Commun.* **2000**, *268*, 384−389.

(69) Wang, L.; Duan, Y.; Stouten, P. F. W.; De Lucca, G. V.; Klabe, R. M.; Kollman, P. A. Does a Diol Cyclic Urea Inhibitor of HIV-1 Protease Bind Tighter Than Its Corresponding Alcohol Form? A Study by Free Energy Perturbation and Continuum Electrostatics Calculations. *J. Comput.-Aided Mol. Des.* **2001**, *15*, 145−156.

(70) Sussman, F.; Villaverde, M. C.; Martinez, L. Modified Solvent Accessibility Free Energy Prediction Analysis of Cyclic Urea Inhibitors Binding to the HIV-1 Protease. *Protein Eng.* **2002**, *15*, 707−711.

(71) Katritzky, A. R.; Oliferenko, A.; Lomaka, A.; Karelson, M. Six-Membered Cyclic Ureas as HIV-1 Protease Inhibitors: A Qsar Study Based on Codessa Pro Approach. *Bioorg. Med. Chem. Lett.* **2002**, *12*, 3453−3457.

(72) Debnath, A. K. Three-Dimensional Quantitative Structure−Activity Relationship Study on Cyclic Urea Derivatives as HIV-1 Protease Inhibitors: Application of Comparative Molecular Field Analysis. *J. Med. Chem.* **1999**, *42*, 249−259.

(73) Debnath, A. K. Comparative Molecular Field Analysis (CoMFA) of a Series of Symmetrical Bis-Benzamide Cyclic Urea Derivatives as HIV-1 Protease Inhibitors. *J. Chem. Inf. Comput. Sci.* **1998**, *38*, 761−767.

(74) Gupta, S. P.; Babu, M. S. Quantitative Structure−Activity Relationship Studies on Cyclic Cyanoguanines Acting as HIV-1 Protease Inhibitors. *Bioorg. Med. Chem. Lett.* **1999**, *7*, 2549−2553.

(75) Gupta, S. P.; Babu, M. S.; Garg, R.; Sowmya, S. Quantitative Structure−Activity Relationship Studies on Cyclic Urea-Based HIV Protease Inhibitors. *J. Enzyme Inhib.* **1998**, *13*, 399−407.

(76) 4.0, J., Schrodinger, Inc. Portland, OR 1991−2000. www.schrodinger.com.

(77) Still, W. C.; Galynker, I. Chemical Consequences of Conformation in Macrocyclic Compounds. *Tetrahedron* **1981**, *37*, 3981−3996.

(78) In this method the ring is opened by breaking a bond between two ring atoms while allowing other ring torsions to vary. After a new set of ring torsions is generated, the bond is closed subject to closure constraints. In this study the minimum and maximum allowable closure distances for 1 were 0.5 and 2.0 Å, respectively. Closure distances outside of these ranges were discarded before minimization.

(79) Ponder, J. W.; Richards, F. M. An Efficient Newton-Like Method for Molecular Mechanics Energy Minimization of Large Molecules. *J. Comput. Chem.* **1987**, *8*, 1016.

(80) Shenkin, P. S.; McDonald, D. Q. Cluster Analysis of Molecular Conformations. *J. Comput. Chem.* **1994**, *15*, 899−916.

(81) Weiner, S. J.; Kollman, P. A.; Case, D.; Singh, U. C.; Ghio, C.; Alagona, G.; Profeta, S.; Weiner, P. K. A New Force Field for Molecular Mechanical Simulation of Nucleic Acids and Proteins. *J. Am. Chem. Soc.* **1984**, *106*, 765.

(82) Kaminski, G.; Friesner, R. A.; Tirado-Rives, J.; W. L. Jorgensen, Evaluation and Reparametrization of the OPLS-Aa Force Field for Proteins Via Comparison with Accurate Quantum Chemical Calculations on Peptides. *J. Phys. Chem* **2001**, *105*, 6474−6487.

(83) Jorgensen, W. L.; Tirado-Rives, J. The OPLS Potential Functions for Peptides. Energy Minimizations for Crystals of Cyclic Peptides and Crambin. *J. Am. Chem. Soc.* **1988**, *110*, 1657.

(84) Hasel, W.; Hendrickson, T. F.; Still, W. C. A Rapid Approximation to the Solvent Accessible Surface Areas of Atoms. *Tetrahedron Comput. Methodol.* **1988**, *1*, 103−116.

(85) Still, W. C.; Tempczyk, A.; Hawley, R. C.; Hendrickson, T. Semianalytical Treatment of Solvation for Molecular Mechanics and Dynamics. *J. Am. Chem. Soc.* **1990**, *112*, 6127−6129.

(86) Qiu, D.; Shenkin, P. S.; Hollinger, F. P.; Still, W. C. The GB/SA Continuum Model for Solvation. A Fast Analytical Method for the Calculation of Approximate Born Radii. *J. Phys. Chem. A.* **1997**, *101*, 3005−3014.
(87) Weiser, J.; Weiser, A. A.; Shenkin, P. S.; Still, W. C. Neighbor-List Reduction: Optimization for Computation of Molecular van der Waals and Solvent-Accessible Surface Areas. *J. Comput. Chem.* **1998**, *19*, 797−808.
(88) Weiser, J.; Shenkin, P. S.; Still, W. C. Approximate Atomic Surfaces from Linear Combinations of Pairwise Overlaps (LCPO). *J. Comput. Chem.* **1999**, *20*, 217−230.
(89) Weiser, J.; Shenkin, P. S.; Still, W. C. Fast, Approximate Algorithm for Detection of Solvent-Inaccessible Atoms. *J. Comput. Chem.* **1999**, *20*, 586−596.
(90) Rao, S. N.; Kollman, P. Simulations of the B-DNA Molecular Dynamics of (Cgcgaattcgcg(2 and D(Gcgcgcgcgc)2: An Analysis of the Role of Initial Geometry and a Comparison of United and All-Atom Models. *Biopolymers* **1990**, *29*, 517−532.
(91) Reddy, R. M.; Erion, M. D.; Agarwal, A.; Viswanadhan, V. N.; McDonald, Q. D.; Still, W. C. Solvation Free Energies Calculated Using the GB/SA Model: Sensitivity of Results on Charge Sets, Protocols and Force Fields. *J. Comput. Chem.* **1998**, *19*, 769−780.
(92) RCSB Protein Databank, www.rcsb.org.
(93) Yamazaki, T.; Hinck, A. P.; Wang, Y.-X.; Nicholson, L. K.; Torchia, D. A.; Wingfield, P.; Stahl, S. J.; Kaufman, J. D.; Chang, C.-H.; Domaille, P. J.; Lam, P. Y. S. Three-Dimensional Solution Structure of the HIV-1 Protease Complexed with Dmp323, a Novel Cyclic Urea-Type Inhibitor, Determined by Nuclear Magnetic Resonance Spectroscopy. *Protein Sci.* **1996**, *5*, 495−506.
(94) The contact criteria is defined as $C =$ (distance between atomic centers)(radius atom 1 + radius atom 2)). Bad contacts were those with a ratio less than 0.89 Å.
(95) Parish, C. unpublished results.

JM049716L